Effectiveness of the Automist Ultra in controlling fire growth

7LS1M0, Masterproject BPS A Research - Q1 & Q2 (2025/2026)

Full Name	Student ID
Inge van Stratum	1810871

Supervisor:
Ir. R.A.P. van Herpen

Eindhoven, February 28, 2026

Contents

Abstract

This study evaluates the effectiveness of the Automist Ultra system in controlling a localised fire. This is essential to enhance safety in elderly care environments, where limited resident mobility and staffing shortages present evacuation challenges. The research focuses on quantifying the system's ability to reduce the Rate of Heat Release (RHR) and establishing its cooling capacity across varying fuel loads and distances. The methodology involved two phases: establishing baseline free-burn RHR curves and conducting suppression tests using wood crib fuel packages (2 and 3 cribs) at distances of 2 and 4 meters from the wall-mounted nozzle. To ensure data accuracy, correction factors for water-uptake and evaporation were applied to isolate the actual pyrolysis mass difference. Effectiveness was determined through slope analysis of the RHR, comparing the suppressed decay phase against the uncontrolled growth curve.

Key results demonstrate that the Automist Ultra significantly reduced the RHR in all tested scenarios. At 4 meters, the system more effectively "capped" the fire's growth despite the extended duration for full extinguishment. Thereby, the cooling capacity increased with both distance and fuel load, rising from 1.00–1.98 kW/s at 2 m to 1.09–2.56 kW/s at 4 m, which suggests a more efficient mist-plume interaction at a higher RHR and larger distances.

The study concludes that while the system is effective for "slow", "medium", and "fast" growing fires, the system may struggle to control "ultra-fast" fires. This is only possible by an ultra fast detection of the fire by a smoke detector or other detection method. These findings provide the RHR data and performance thresholds required for future tests and simulations to determine the maintenance of tenable conditions during evacuation.

1 | Introduction

This study was initiated in response to growing concerns about fire safety in elderly care homes. There is a demand to extend the available escape time and reduce the amount of staff required for evacuation during a fire emergency. This results from the challenge of the residents' often limited mobility and the shortage of manpower. At the same time, the increased presence of mobility scooters and other battery powered devices creates a risk of lithium-ion battery fires. These types of fires differ from conventional fires by not requiring oxygen to sustain combustion. Traditional fire safety systems may therefore not perform as effectively as for a "normal" fire. This had led to the question whether the Automist Ultra system can control, delay or extinguish battery fires. While it is crucial to determine whether the Automist system can control or delay such incidents, the system is not tested for battery fires in this research. First, the fundamental capabilities and limitations of the system must be defined according to the following research questions:

1. **To what extent can the Automist Ultra system reduce the Rate of Heat Release (RHR) of a developing fire of different fuel loads?**
2. **Is the Automist uniformly effective over varying distances from the nozzle?**
3. **How effective is the Automist in practice when using design RHR curves related to residential functions?**

This study focuses on quantifying the effectiveness of the Automist in reducing the Rate of Heat Release (RHR) using wood crib fuel packages. The research is structured into two phases. First, establishing a baseline RHR curve through uncontrolled free-burn tests of the fuel packages. Secondly, performing suppression tests to quantify the Automists' impact on the RHR curve across varying distances from the system.

Furthermore, this paper details the data processing methodology required to produce accurate results. This involves integrating data over an interval to account for noise from high-pressure spraying and applying correction factors to account for both the uptake and evaporation of water.

The final goal of this research is to establish the cooling capacity of the Automist and translating this into practical applications with the standard t-squared fire growth curves. Defining how the Automist performs is essential for future research regarding more complex fire types, such as those involving lithium-ion batteries.

2 | Literature Review

This section is structured to first define the operational principles of the Automist Ultra. After which it describes existing research and case studies to summarize how the system has performed in standardized tests and computational simulations.

2.1 | Automist Ultra

The Automist Ultra system is a watermist system, however, instead of ceiling heads it uses wall-mounted nozzles. These are connected to a high-pressure pump which is supplied by the domestic water supply, see Figure 2.1b. So, the water inlet of the pump is the normal drinking water system of the residential function. This pump can supply up to 10 nozzles. With the high-pressure pump, the nozzle achieves a water discharge rate of 8.4 L/min with a spray pressure between 75 up to 90 bar. It is a relatively new system designed for domestic use (houses and apartments). The Automist works as follows; The system is activated by a wired smoke detector after which an infrared (IR) sensor (750 pixels) scans the room. The IR-sensor is located within the nozzle head that is mounted to the wall at 1.12 m to 1.3 m. During scanning, the IR sensor measures the temperature as a function of IR radiation. When the temperature increase with time exceeds a certain threshold between scans, the nozzle has located a fire. The nozzle starts spraying small water droplets (mist) in the direction of the fire, thereby cooling the surroundings and reducing the availability of oxygen in the immediate vicinity of the fire. The nozzle has a fire-tracking algorithm that continuously monitors the location of the fire, Figure 2.1a. If the fire shifts to a different position, the system stops mist discharge, re-scans the room to determine the relocated fire, and then resumes mist discharge oriented towards the new fire area [2][8][11].

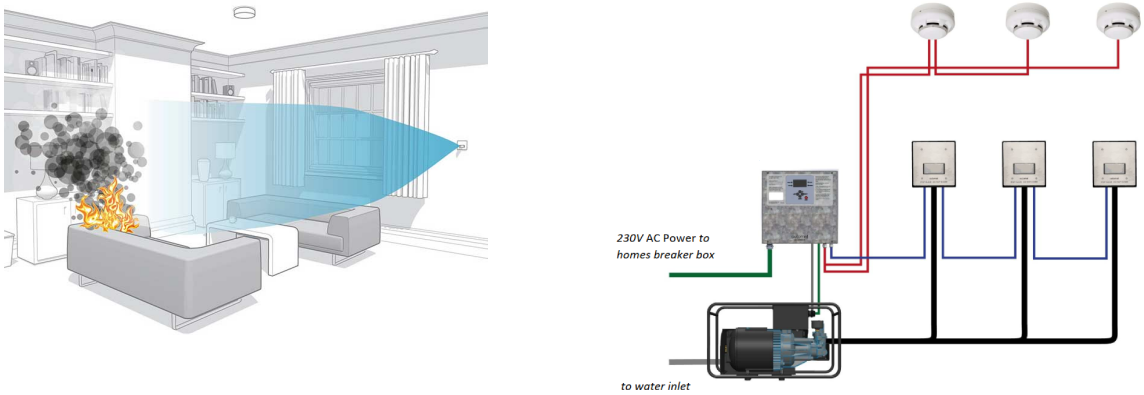

(a) Automist in action [14] **(b)** System diagram [12]

Figure 2.1: The Automist Ultra System

2.2 | Existing research

There are two versions of the Automist, the Hydra version, and the Ultra version. In concept, they are very similar. The Hydra version is sold since 2019 in the UK. In 2024, the Ultra version was launched. The new version is faster at finding the fire and has a fire tracking algorithm [11]. In 2019 the Automist was introduced by Plumis as a response to calls for fire sprinkler innovation, especially for domestic use. The activation time of the Automist is up to 13.7 times quicker than a sprinkler system in many scenarios. This is mainly because the system activates before the required temperature to burst the glass bulb of a sprinkler is reached [10]. This fast response means that less water is needed for suppressing a fire than in a normal sprinkler system.

Plumis is a British company, therefore, the product is developed and tested in accordance with the British Standards (BS) in March 2022. Specifically, the Automist Hydra is tested in line with Annex C which describes 8 test set-ups evaluating the effectiveness of a fire suppression system. The fire tests focusses on the thermocouple temperatures observed at 75mm from the ceiling (max. 320 °C) and 1.6m above

floor level (max. 95°C or 55°C for not more than any 120 s interval) [7]. The Automist Hydra succeeded these tests, it complies with the clause for domestic premises at a maximum room size of 80 m^2 and maximum ceiling height of 3.5 m [1]. However, these tests only focus on thermocouple temperatures so the suppression performance with respect to the RHR (Rate of Heat Release) is not quantified.

In September 2022, a study evaluated the performance level of several modelling approaches to represent the suppression behaviour of the Automist Hydra, based on the test results obtained from the BS. The compared models were a capped fire, Nystedt, and Evans model. The Evans exponential decay model provided the best overall agreement with the experimental data, particularly when an equivalent sprinkler spray density of 0.07 mm/s was adopted. However, it should be noted that the simulations only cover a limited range of fire scenarios [7].

A later study performed in November 2022 used the previous research as input parameters for a simulation model with a building that deviates from the guidance of the BS. The model exists of a three-storey open-plan dwelling house with an open stairway. With this, the study investigates the performance of Automist Hydra in a open plan situation compared to a conventional protected-stair or sprinkler protected design. The study concluded that the Automist Hydra system can achieve a performance equivalent to or even exceeding the minimum expectations for a domestic sprinkler system, with fewer incidents of injury or fatality. It is therefore reasonable to adopt the Automist Hydra system where the design deviates from the guidance recommendations. However, the report notes that de modelling only covers a limited range of fire growth scenarios, dwelling arrangements and behavioural assumptions [5].

Since the Automist Hydra is a recent innovation, it faces challenges in obtaining a certification because existing standards are not directly applicable. In those cases, a product needs to be verified both by testing with relevant standards and a comprehensive review of the product's technical aspects. When these assessments are successful, The British Standards Institution (BSi) can issue a BSi Verification Certificate [13]. In 2023, the Automist Smart scan Hydra system retrieved such a certificate since it has been independently, third-party, tested by Exova Warrington Fire to confirm that it meets the performance requirements of BS [16].

A documented case study by Plumis describes a residential fire incident in June 2023 in Greater Manchester, where an Automist Smart Scan Hydra system was installed in an open-plan kitchen area. The incident involved a chip pan fire that broke out after the occupant left cooking oil unattended on the stove. Within approximately 21 seconds of smoke detection, the system identified the fire source and began mist discharge. The fire was fully extinguished after about 10 minutes, using about 60 Liters of water. There were no injuries and minor smoke damage was reported [6].

Next to the BS, a smart device can retrieve an UL mark. This indicates that a product has been through rigorous testing by Underwriters Laboratories. The UL safety Mark means that a product has been certified to meet national scientific safety, quality or security standards [15]. The Automist Hydra version complies with the BS, however, it is not UL-listed. The new Ultra version meets all the extra requirements and is therefore UL-listed [11].

The Automist Ultra is tested following the UL Subject 2167, which is the standard for water mist nozzles for fire protection service released in 2011. This standard is being reviewed and a new version will be released in 2026. To be prepared for the new version, the Ultra version was already tested for the draft version of the UL 2167B in 2023. The UL-tests include 16 full-scale fire tests across small and large rooms with fabricated sofas, drapes, combustible walls, cooking oil fires, (un)obstructed scenarios, and multiple nozzle placements (far wall, near wall, multi-nozzle configurations). The most important criteria are;

- The maximum peak temperature at 1.60m cannot exceed 93.3°C (200°F).
- The temperature at 1.60m above floor cannot exceed 54.4°C (130°F) for more than 120 seconds.

In all sixteen fire tests, the results show that the Automist Ultra system successfully maintained temperatures within defined safety limits. It is important to note that due to the draft nature of the requirements the applicability of test data is not guaranteed, and further testing may be required [3].

3 | Method

The testing phase was divided into two steps. The first phase consisted of conducting a fully burn of the selected fuel package to measure a baseline RHR curve against which follow-up tests could be compared. In the second phase, the effectiveness of the Automist Ultra was tested by conducting fire tests using different fuel packages and varying distances from the nozzle. These experiments were designed to assess the influence of the Automist system on the RHR curve.

3.1 | Fuel Package

For the fire tests, 2 fuel packages were used with varying fire loads. Both packages consist of multiple wood cribs with a dimension of 0.30mx0.30mx0.11m (LxWxH). One wood crib has 30 uniformly sized timber members arranged in a regular stacked configuration. The crib has 5 layers with 6 members placed parallel to each other, each layer is placed orthogonally on top of the other one. This forms a cross-stacked structure that enhances uniform air entrainment throughout the crib. A detailed visual of the wood crib can be seen in Figure 3.1a.

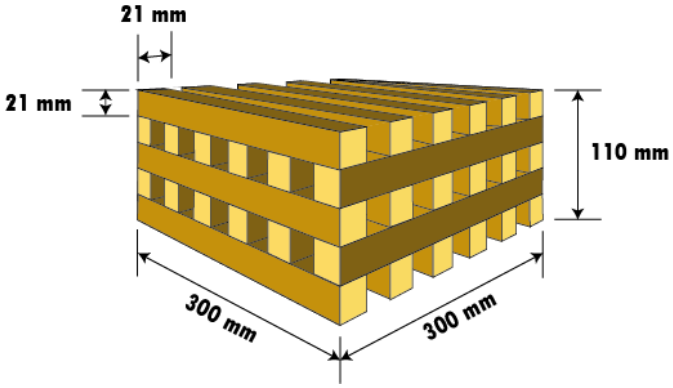

(a) Wood Crib

(b) Wood cribs used in experiments

Figure 3.1: Wood Cribs

One wood crib has a weight of 2.0974 kg. The two fuel packages differ in fuel load by differing the amount of wood cribs, the properties of the two fuel packages are described in Table 3.1.

Table 3.1: Properties of fuel packages

Fuel package	Amount of Cribs	Total Energy (kJ)
Package 1	2	79,701
Package 2	3	119,552

3.2 | Baseline Fire Test

The baseline fire test was conducted in the fire safety laboratory Peutz in Haps. In this test, the fuel package was allowed to burn freely. This scenario represented an uncontrolled fire development. The fuel packages was placed at the centre of a weight measuring device, allowing continuous measurement of mass throughout the test. The set-up was placed under a ventilation hood to remove smoke and combustion gases. Ignition was initiated using 8 kerosene fire starter blocks (1 cm^3 each). After ignition, the fire was allowed to develop until the fuel package was fully consumed. Each second, the mass was recorded by a data logger.

The test was performed for both fuel packages and repeated 2 times to confirm repeatability. The averaged baseline RHR curve was used for comparison with the suppression tests.

3.3 | Suppression Tests

For all suppression tests, the test chamber located at Aqua+ in Goor was used. This room is equipped with an Automist Smartscan Ultra system with 2 nozzles, located at 1.2 m above floor level. A smoke detector to activate the system, located in the corner of the room, and a temperature meter in the middle of the room. The test chamber has a surface area of 24.5 m^2 and a height of 2.4 m. The parameters of the test chamber can be seen in Figure 3.2.

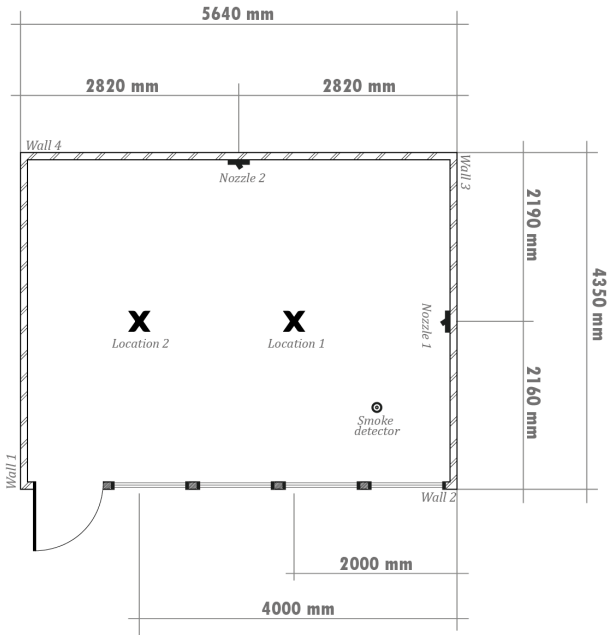

Figure 3.2: Test chamber Aqua+

During the suppression tests, only Nozzle 1 was considered for the analysis. Nozzle 2 was covered to make it inactive. To ensure that the wood crib reached the desired fire load before the activation of the Automist. The system was disconnected from the smoke detector and was therefore activated manually. This procedure allowed for a controlled and repeatable test environment.

The suppression tests were performed using two different fuel packages positioned at two distances from the nozzle. Location 1 was situated 2 m from the nozzle, while Location 2 was located at a doubled distance of 4 m. In all tests, the fuel packages were positioned at 1 m above floor level.

Figure 3.3: Test set-up

Each fuel package was placed on a scale connected to a data logger to continuously record mass difference during the test. Every test was performed 3 times to ensure consistency. The test set-up for the suppression tests is shown in Figure 3.3. The figure shows the following elements from bottom to top; a raised platform, the measurement scale connected to the data logger, a protective tray, and the wood cribs. Because of the tray in which the wood cribs were placed, the results needed to be corrected on water uptake caused by both the wood crib absorbing water and the tray catching water. Thereby, due to the high temperature of the fire, a part of the water which was taken up evaporates.

How these correction factors were established and applied is described in subsection 3.5.

3.4 | Water Uptake Test

To measure the mass increase resulting from water uptake, additional tests were performed without igniting the fuel package while still activating the Automist system. The fuel packages were placed on the test setup, after which the Automist system was activated three times for a duration of 1 minute each, resulting in a total activation time of 3 minutes. The data was logged accordingly and used to correct the suppression test data for mass increase due to the water uptake.

3.5 | Data Processing

The raw data retrieved from the suppression tests consists of the total mass measured every second, which allows for the calculation of the mass loss rate per second. To transform the RHR data into a reliable curve, multiple processing steps were required to account for experimental noise, water interaction, evaporation, and the limitations of the fuel packages.

The mass loss rate was used to determine the RHR according to Equation 3.1.

$$Q = m_{loss} \times \Delta H_c \qquad [\text{kW}] \tag{3.1}$$

Where Q is calculated in kilowatts (kW), m_{loss} is the the rate of mass loss in kg/s, and ΔH_c is the heat of combustion, which is 19,000 kJ/kg for the wood cribs. This value represents the heat released during the oxidation process of the fuel [4][18].

However, Equation 3.1 does not account for the simultaneous mass increase caused by water uptake from the Automist system and the mass loss resulting from water evaporation during active fire suppression. Without corrections, the results show an overestimation of the RHR. To address this, the results were corrected using a mass balance that accounts for the different components of the measured weight as described in Equation 3.2.

$$\frac{dm_{\text{pyro}}}{dt} + \frac{dm_{\text{water}}}{dt} + \frac{dm_{\text{evap}}}{dt} = \frac{dm_{\text{total}}}{dt} \qquad [\text{kg/s}] \tag{3.2}$$

Where m_{total} is the total mass change measured during fire suppression tests, m_{pyro} is the actual mass loss of the fuel (wood cribs) due to pyrolysis, m_{water} is the constant mass increase from the Automist system, measured during the water uptake tests without a fire, and m_{evap} is the mass of water that evaporates due to the heat of the fire.

To calculate the actual pyrolysis mass loss, the energy balance must be considered. The heat of combustion for the fuel (H_c) is 19,000 kJ/kg. The energy required for water evaporation is 2,600 kJ/kg (based on the latent heat of water). By combining the energy and mass balances, the evaporation correction factor was derived, which is elaborated in Appendix A. From this combination, also the formula to calculate the mass loss only due to pyrolysis was retrieved, which is Equation 3.3.

$$\Delta m_{pyro} = 0.12 \times (\Delta m_{total} - \Delta m_{water}) \qquad [\text{kg/s}] \tag{3.3}$$

The actual RHR (RHR_{pyro}) was determined using Equation 3.4, using the corrected mass loss and the heat of combustion (H_c).

$$RHR_{pyro} = \Delta m_{pyro} \times 19,000 \qquad [\text{kW}] \tag{3.4}$$

The raw data (m_{total}) was retrieved at a one-second interval. While this provided detailed measurements, the high-pressure discharge from the Automist nozzle introduced significant noise into the mass measurements. To produce a stable RHR curve, the results were moving averaged over 60 seconds. The resulting graphs showed that the noise was sufficiently reduced which allowed for a clearer analysis of the system's effectiveness.

3.6 | Effectiveness

The effectiveness was defined as the cooling capacity of the Automist system at a specific RHR. This cooling capacity was calculated by comparing the "with" and "without" suppression scenarios based on slope analysis. This returned into 4 data points (from the four scenarios) which were extrapolated to relate the results to bigger RHR values. However, for this extrapolation is a maximum RHR that can reliably be extrapolated. A rule-of-thumb is that the energy from the fire should not cause more than 10% of the water flow to evaporate. The energy required to evaporate water is approximately 2.4 MJ/kg (L_v). With the calculated evaporation of water which was described in previous sections, the maximum thermal power that can be absorbed by the water flow was calculated.

To translate the cooling capacities into practical values, the performance of the system was evaluated against standard design scenarios used in performance based fire safety analyses (slow $t_c = 600$s, medium $t_c = 300$s, fast $t_c = 150$s, ultra fast $t_c = 75$s) [17]. For the Automist system to effectively cap or extinguish a developing fire, the growth rate in kW/s (represented by the tangent of the fire growth curve) may not exceed the determined cooling capacity.

In the baseline fire tests (subsection 3.2), the fuel packages had a limited total energy content of 79,701 kJ for two cribs and 119,552 kJ for three cribs. This resulted in a reference curve with a peak followed by a decay phase as the fuel was exhausted. However, for the analysis, a non-decaying reference curve was required. This was created by using the measured data and extrapolate that into a growing curve. To ensure the theoretical curve takes over smoothly from the actual fire growth data, the alpha (α) based on the peak intensity reached before the fuel is exhausted was calculated using Equation 3.5 [9].

$$\alpha = \frac{\text{Peak RHR}}{\text{t}^2} \qquad [\text{kW/s}^2] \tag{3.5}$$

During the time before the peak, the measured RHR values were used, as these represent the actual observed growth. For the time after the peak, instead of using the decaying values, Equation 3.6 was used.

$$RHR = \alpha \times \text{t}^2 \qquad [\text{kW}] \tag{3.6}$$

This theoretical increasing curve represents an uncontrolled fire with an unlimited fuel supply. The cooling capacity was then calculated as the average difference in slope between the suppressed and free-burn scenario 30 seconds after the activation of the Automist.

4 | Results

The results show the performance of the Automist system across four distinct scenarios involving varying distances (2m and 4m) and fuel loads (2 and 3 wood cribs). The data gathered demonstrates the system's ability to control and extinguish developing fires compared to uncontrolled reference curves.

4.1 | Water Uptake Test

The water uptake tests showed a consistent water output of the Automist system which reached the fuel package. The applied correction factors for each scenario are as shown in Table 4.1.

Table 4.1: Correction factors water uptake

Distance to Nozzle	Fuel Package	Correction Factor
2 m	1	0.019
	2	0.026
4 m	1	0.005
	2	0.006

The graphs of the measured data can be found in Appendix B. The results showed that the water uptake is significantly less when the distance is increased with a difference in correction factor of 0.014 up to 0.020.

4.2 | Evaporation

For the evaporation correction factor, both the mass balance and the energy balance as described by Equation 3.2 and Equation 3.4 respectively, were used. The complete calculation is described in Appendix A. A correction factor of 0.12 kg/s was retrieved. This factor was applied to the measurement results only after the activation of the Automist.

4.3 | Fire Suppression Tests

The retrieved data, calculated from mass loss every second, showed the effect of the Automist system on the RHR curve. The four scenarios were subjected to three suppression tests (Test 1, 2, and 3), which were then compared to the baseline free-burn scenario (Reference). Figure 4.1 and Figure 4.2 show the influence of the Automist on the RHR curve of the 4 scenarios, corrected on water uptake and evaporation.

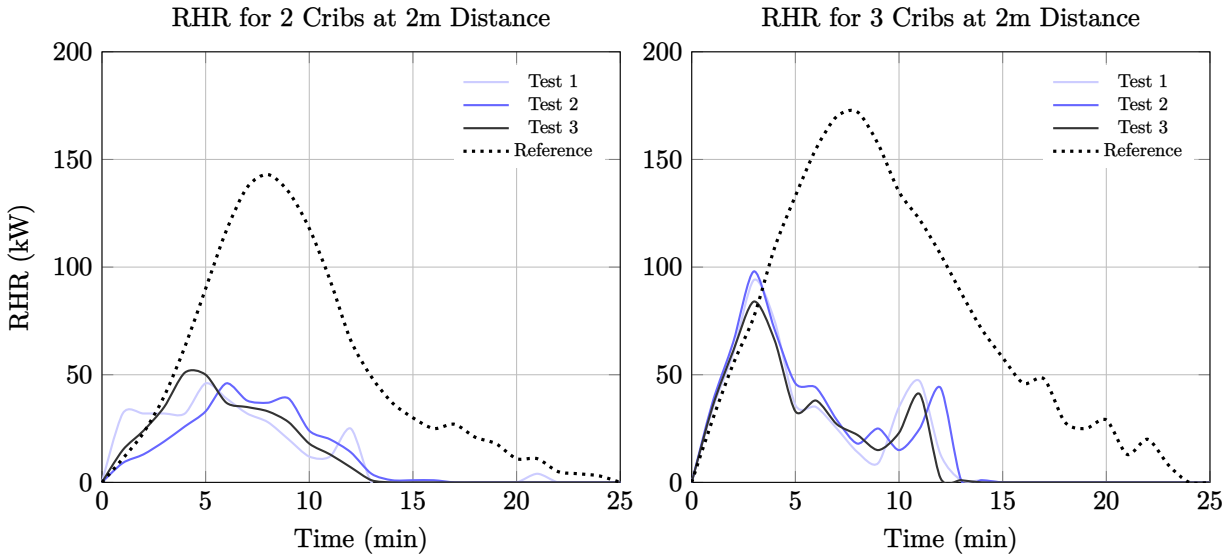

Figure 4.1: RHR over time at a 2-meter distance with varying fuel loads.

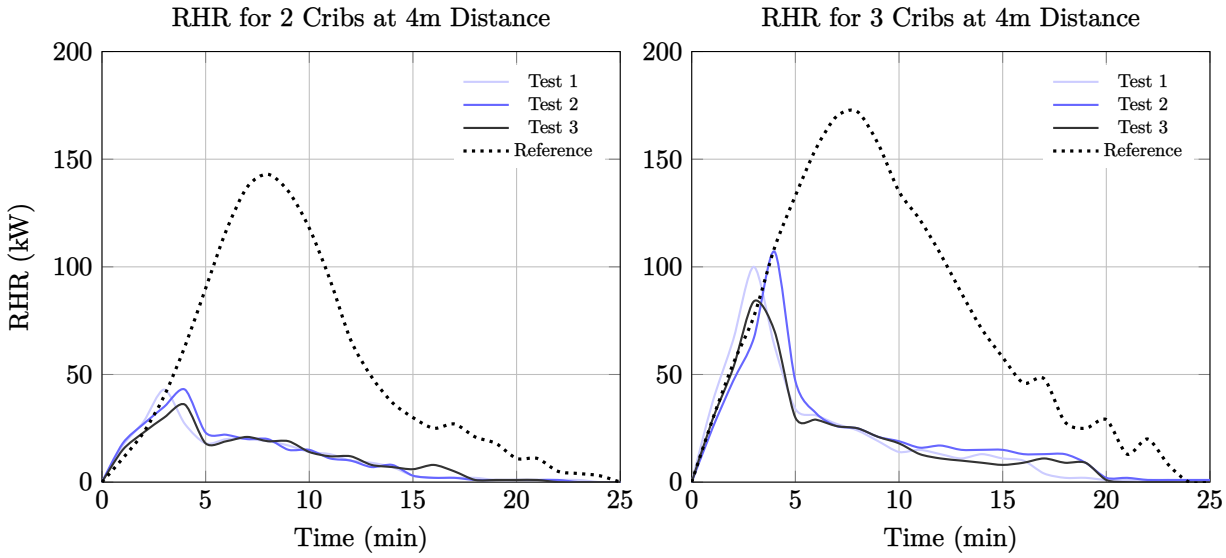

Figure 4.2: RHR over time at a 4-meter distance with varying fuel loads.

At both distances, once the Automist system was activated, the fire entered a decay phase. At 4 meters, the fire was quickly controlled and entered a more stable decay phase than for the 2 meter distance. However, the duration was notably extended. Thereby, the addition of a third crib resulted in a higher RHR peak at activation by approximately 60 kW compared to the 2-crib fuel packages, however, the fire growth (slope) stayed approximately the same.

4.4 | Effectiveness

For the effectiveness of the Automist the slope of the non-suppressed graph was calculated and was compared to the slope of the suppressed graph 30 seconds after activation. This resulted in a difference which was translated into cooling capacities. Figure 4.3 shows the RHR for test 2 at a distance of 4 meter with fuel package 2.

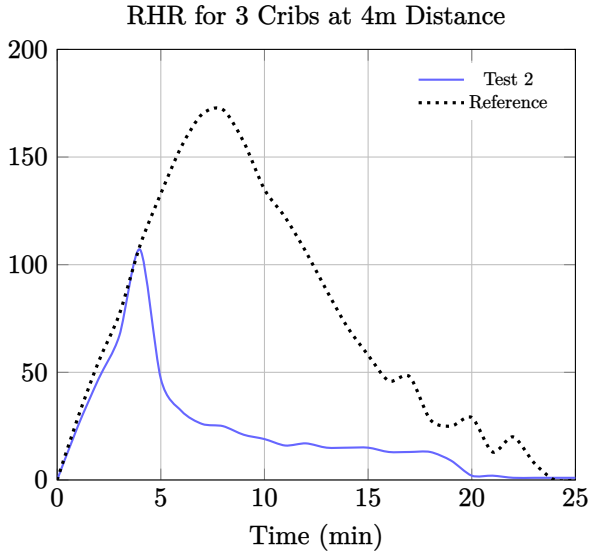

Figure 4.3: RHR of test 2 over time at a 4-meter distance with fuel package 2.

The figure shows that the results of test 2 follow the reference curve until a given point at around 4.5 minutes, which is the activation of the Automist. The cooling capacity was derived from the difference of the tangent of the reference RHR curve and tangent of the retrieved data RHR curve.

By calculating the average difference between these two slopes for a duration of 30 seconds after activation, the system's ability to remove energy from the fire is quantified in kW/s. Which can be described as the cooling capacity.

For the Automist to successfully control the fire, the calculated cooling capacity must exceed the growth rate of the fire at the moment of activation. This relationship between the two slopes determines whether the fire is successfully turned into a decay phase or continues to grow.

The slope of the non-suppressed graph (Reference) was 0.42 kW/s for fuel package 1 and 0.43 kW/s for fuel package 2. These values were compared to the slopes of the suppression tests and cooling capacities, shown in Table 4.2, were derived together with the RHR at the time of activation.

Table 4.2: Cooling capacity Automist

Fuel Package	Distance	Cooling capacity average [kW/s]	Range [kW/s]	RHR [kW]
1	2	1.00	0.79 - 1.15	56
	4	1.09	0.86 - 1.34	44
2	2	1.98	1.74 - 2.34	102
	4	2.56	2.26 - 3.00	114

Table 4.2 shows that the cooling capacity increases with higher fuel loads with a higher RHR development. For instance, at a 4-meter distance, the cooling capacity increased from 1.09 kW/s for 2 cribs to 2.56 kW/s for 3 cribs. Thereby, for both fuel packages, the cooling capacity increases with an increasing distance from the nozzle. The relation between cooling capacity and RHR is shown in Figure 4.4. The maximum reliable RHR extrapolation was calculated with the rule of thumb stated in subsection 3.6.

$$RHR_{max} = m_{evap} \cdot L_v = 0.120 \text{ kg/s} \cdot 2.4 \times 10^6 \text{ J/kg} = 2.88 \times 10^5 \text{ W} \approx 288 \text{ kW} \tag{4.1}$$

The graph shows the cooling capacity with respect to the RHR for both fuel loads and both distances. The four scenarios are shown as a circle with a white fill, the average data of the measurements with the same fuel load but varying distances are shown as black dot. This eliminates the element of the distance to the nozzle from the measurement results. While this parameter might have an affect on the cooling capacity, the distance to the nozzle is assumed to be insignificant for the cooling capacity in this graph.

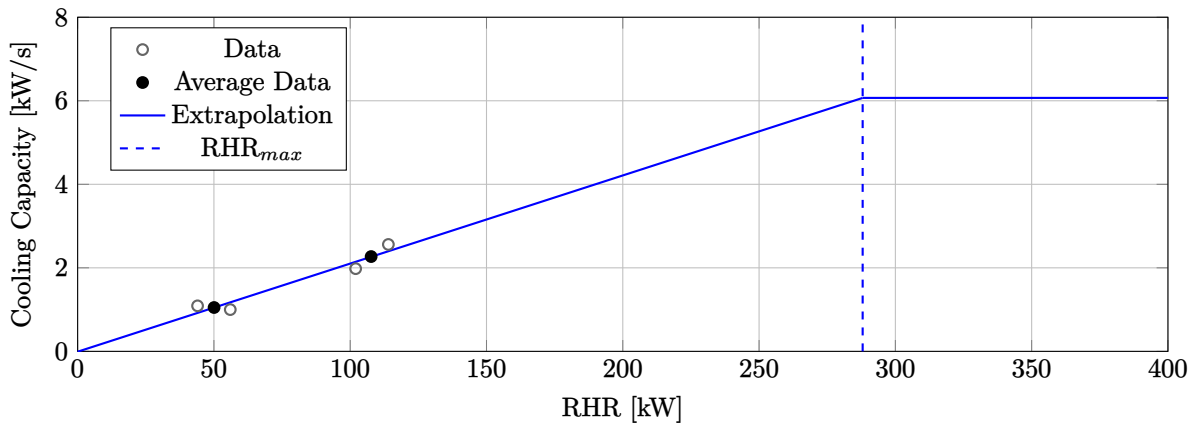

Figure 4.4: RHR vs Cooling Capacity with Trendline

The two averaged data points show an upward trend in cooling capacity with an increasing RHR. This trend is extrapolated until the calculated RHR_{max} from Equation 4.1. The graph shows that the cooling capacity can be (safely) extrapolated up until a value of 6 kW/s.

For more practical values, the maximum cooling capacity was compared against the standard t-squared curves. The effectiveness of the Automist Ultra was determined by the relationship between the fire's growth rate and the system's established maximal cooling capacity. Mathematically, the cooling capacities are defined as the derivative of the fire growth curve after activation (t_{act}). With the condition that for the Automist to successfully cap or extinguish a fire, this growth rate must not exceed the cooling capacity of the Automist.

By applying this condition to the standard fire growth curves (slow, medium, fast, and ultra-fast), the time frame within which the Automist needs to begin discharging water (t_{act}) can be calculated for each growth curve.

The maximum allowable time for system activation was determined and is shown in Figure 4.5 for each growth curve. Also shown are the theoretical extrapolated curves for the 2- and 3-crib fires.

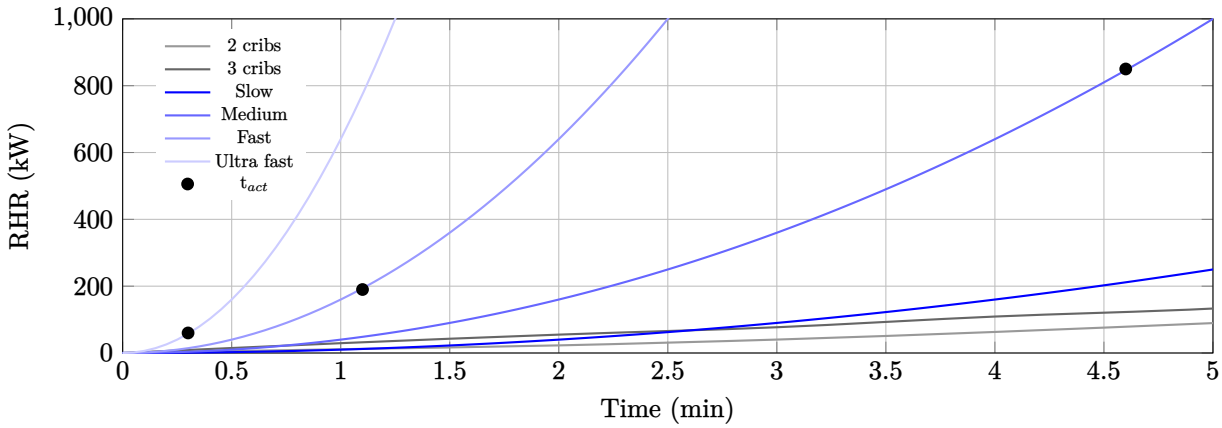

Figure 4.5: T-squared growth curves

Not shown in Figure 4.5 is the activation time for the "slow" developing fire, this is at t = 18.2 minutes. The exact activation time in seconds for each growth curve can be found in Table 4.3.

Table 4.3: Activation for a cooling capacity of 6 kW/s

Fire Growth Curve	Slow	Medium	Fast	Ultra Fast
Activation time [s]	1080	270	68	17

If the activation time of the Automist is higher than the numbers presented in the table, the fire will continue to grow uncontrolled despite the suppression of the Automist. The table shows that for an ultra-fast fire growth, the activation time of the Automist needs to be within 17 seconds. For the other cases, the activation time can be after 1 minute.

5 | Discussion

The results show that the Automist Ultra system is effective at controlling and suppressing developing fires across varying scenarios. This section discusses the influence of distance, fuel load, and operational limitations on the system's performance.

The data processing phase was critical for isolating the actual fire behaviour. The high-pressure discharge (75–90 bar) introduced significant noise into the mass measurements results. Integrating the data over a 60-second timestep was needed to filter this noise and show the true RHR trends. Thereby, the results initially overestimated the RHR due to the simultaneous effects of water uptake and evaporation. By applying the derived correction factors, the mass loss solely due to fuel pyrolysis was retrieved. This ensured accurate and reliable RHR data with which further analysis could be done.

It was found that the distance between the nozzle and the fire source alters the suppression graph. Both fires enter a decay fase relatively quickly after activation. However, at the 4-meter distance, the system appears to more effectively cap the fire. Although the total duration required for full extinguishment is extended at the 4-meter distance. This also shows in the data of the cooling capacity which increases with distance for both fuel loads. For instance, the average cooling capacity for 3 cribs rose from 1.98 kW/s at 2 m to 2.56 kW/s at 4 m. This suggests that at greater distances, the Automist achieves a better distribution of the mist and can interact better with the fire.

As expected, the addition of a third wood crib increased the peak RHR at time of activation (by approximately 60 kW) compared to the 2-crib packages. While the fuel load was increased, the Automist system successfully achieved extinguishment in all tested scenarios. A key finding resulting from this is that the cooling capacity of the Automist increases with higher fuel loads. This trend suggests that when a fire has a bigger rate of heat release, the Automist can more efficiently interact with the fire. This shows a better (and robust) performance for larger loads.

The results show that the cooling capacity of the Automist is not only related to slope of the RHR curve but also on the magnitude of the RHR at the time of activation. There is a clear correlation between an increased fuel load and an increased cooling capacity. The successful suppression of fuel package 2 (3 wood cribs) shows that the Automist has not reached its physical performance boundary yet, so extrapolation could be performed, but with caution since the cooling capacity is not unlimited. Given that the measured cooling capacity trended upward with larger loads, the cooling capacity was extrapolated to 6 kW/s for a RHR of 288 kW. However, the maximum fuel load the Automist can suppress was not tested in this research and remains unknown.

Furthermore, the analysis against standard t-squared growth curves showed that for the maximal cooling capacity of 6 kW/s, the system can be activated after a minute and still be effective in most cases. However, for the ultra-fast fire growth curve, the system would need to activate in under 60 seconds to be effective. Here, the practical application of the Automist starts playing a role. The effectiveness of the Automist is constrained by its activation and scanning. The Automist is dependent on a wired smoke detector for activation, followed by an infrared scan of the room to locate the fire, which takes approximately 9 seconds. For this process to happen within 60 seconds is considered unlikely. For situations where an ultra fast fire development would be expected, another form of fire detection could be implemented into the system.

6 | Conclusions

This research quantified the effectiveness of the Automist Ultra system in controlling and suppressing developing fires across varying scenarios. By comparing uncontrolled free-burn tests with suppression trials, the study established an understanding of the system's impact on the Rate of Heat Release (RHR). The study found interesting conclusions for the following research questions:

To what extent can the Automist Ultra system reduce the Rate of Heat Release (RHR) of a developing fire of different fuel loads?

- The Automist Ultra significantly reduced the RHR in all tested scenarios compared to uncontrolled baseline curves. For the greater distance (4 meter), the system was found to more effectively cap the fire growth. However, full extinguishment required a longer time duration than for the shorter distance (2 meter).

Is the Automist uniformly effective over varying distances from the nozzle?

- Suppression performance is not uniform across varying distances. Actually, the cooling capacity increased with distance, rising from 1.00–1.98 kW/s at 2 m to 1.09–2.56 kW/s at 4 m. Furthermore, a positive correlation was found between fuel load and cooling capacity, suggesting that the system's interaction with the fire plume becomes more efficient as the RHR increases.

How effective is the Automist in practice when using design RHR curves related to residential functions?

- The system was considered effective only if it starts discharging water before the fire's growth rate exceeds the cooling capacity of the Automist Ultra. It was found that for "slow", "medium", and "fast" developing fires, the activation time is well within the capabilities of the Automist Ultra. However, an "ultra-fast" developing fire requires an activation within 17 seconds, which is considered unlikely.

In summary, the Automist Ultra provides a robust suppression capability for varying fires, potentially extending available evacuation time in elderly care environments. These results provide the necessary cooling capacity thresholds and RHR data for the follow-up research where bigger fuel loads or even battery fires can be tested and simulated to determine their tenable conditions.

7 | References

[1] E. Anderson. Method for measuring the capability of a watermist system to control a fire - "room fire tests for watermist systems with automatic nozzles". Technical report, 2022.

[2] Aqua+. Automist: Brandpreventie thuis, 2025. https://www.aqua.nl/oplossingen/automist.

[3] Christopher Dostal. Preliminary investigation for fire testing of plumis model sh12_ae smartscan multiroom spray head, non-automatic (open) type water mist nozzles. Technical report, UL Solutions, April 2023.

[4] D. Drysdale. Fire science and combustion. In *An Introduction to Fire Dynamics*, chapter 1. John Wiley & Sons, 3rd edition, 2011.

[5] Ashton Fire. Probabilistic modelling of open plan dwellinghouses. November 2022.

[6] Plumis Ltd. Fire incident report summary. June 2023.

[7] Y. Muhammad M. Spearpoint, C. Hopkin and W. Makant. Estimating the suppression performance of an electronically controlled residential water mist system from bs 8458:2015 fire test data. *Fire*, 2022.

[8] Y. Muhammad M. Spearpoint, C. Hopkin and W. Makant. Replicating the activation time of electronically controlled watermist system nozzles in b-risk. *Fire Safety Journal*, 130:103592, 2022.

[9] Dr. Kris Overholt. Fire ramp calculator. Technical report, University of Texas at Austin Mechanical Engineering, N.D.

[10] Plumis. Why do we need fire sprinkler innovation?, 2020. https://plumis.com/calls-innovation.

[11] Plumis. Automist product versions. Technical report, Plumis, 2024.

[12] Plumis. Design, installation, operation and maintenance (diom) manual. Technical report, 2024.

[13] Plumis. Does automist comply with the guidance within the associated british standard? Technical report, 2024.

[14] Plumis. Why automist, 2025. https://plumis.co.uk/why-automist.

[15] UL Solutions. Look for the ul safety mark before you buy, 2025. https://www.ul.com/look-ul-safety-mark-you-buy.

[16] BSI Assurance UK. Bsi verification certificate. Technical report, 2023.

[17] Guan-Yuan Wu and Ruu-Chang Chen. The analysis of the natural smoke filling times in an atrium. January 2010.

[18] Trent Parker Qingsheng Wang Zeren Jiao, Harold U. Escobar-Hernandez. Review of recent developments of quantitative structure-property relationship models on fire and explosion-related properties. September 2019.

A | Appendix A — Evaporation Correction Factor

To calculate the evaporation correction factor which needs to be applied to the mass change measured during the fire suppression tests, both the mass balance and energy balance are required. Below, it is shown step by step how the correction factor is retrieved.

Mass Balance:

$$\frac{dm_{\text{pyro}}}{dt} + \frac{dm_{\text{water}}}{dt} + \frac{dm_{\text{evap}}}{dt} = \frac{dm_{\text{total}}}{dt} \tag{A.1}$$

$$\Delta m_{pyro} + \Delta m_{water} + \Delta m_{evap} = \Delta m_{total} \qquad [\text{kg/s}] \tag{A.2}$$

Energy Balance:
Pyrolysis:

$$RHR_{pyro} = \frac{dm_{\text{pyro}}}{dt} \times -19,000 \qquad [\text{kW}] \tag{A.3}$$

$$\Delta m_{pyro} = \frac{RHR_{pyro}}{-19,000} \qquad [\text{kg/s}] \tag{A.4}$$

Evaporation:

$$RHR_{pyro} \geq \Delta m_{evap} \times -2,600 \qquad [\text{kW}] \tag{A.5}$$

Combine Equation A.4 with Equation A.5

$$\Delta m_{pyro} = \frac{\Delta m_{evap} \times -2,600}{-19,000} \qquad [\text{kg/s}] \tag{A.6}$$

$$\Delta m_{evap} = \Delta m_{pyro} \times \frac{19}{2.6} \qquad [\text{kg/s}] \tag{A.7}$$

Combine Equation A.2 with Equation A.7

$$\Delta m_{pyro} + \Delta m_{water} + \Delta m_{pyro} \times \frac{19}{2.6} = \Delta m_{total} \tag{A.8}$$

$$\Delta m_{pyro} = \frac{2.6}{21.6} \times (\Delta m_{total} - \Delta m_{water}) \qquad [\text{kg/s}] \tag{A.9}$$

So the correction factor for evaporation is $\frac{2.6}{21.6}$, which is 0.12.

B | Appendix B — Water Uptake Tests Results

In the figures below, the water uptake of the four scenarios without ignition is shown. Mind that the y-axis for the different amount of cribs vary, while it stays the same for varying distances.

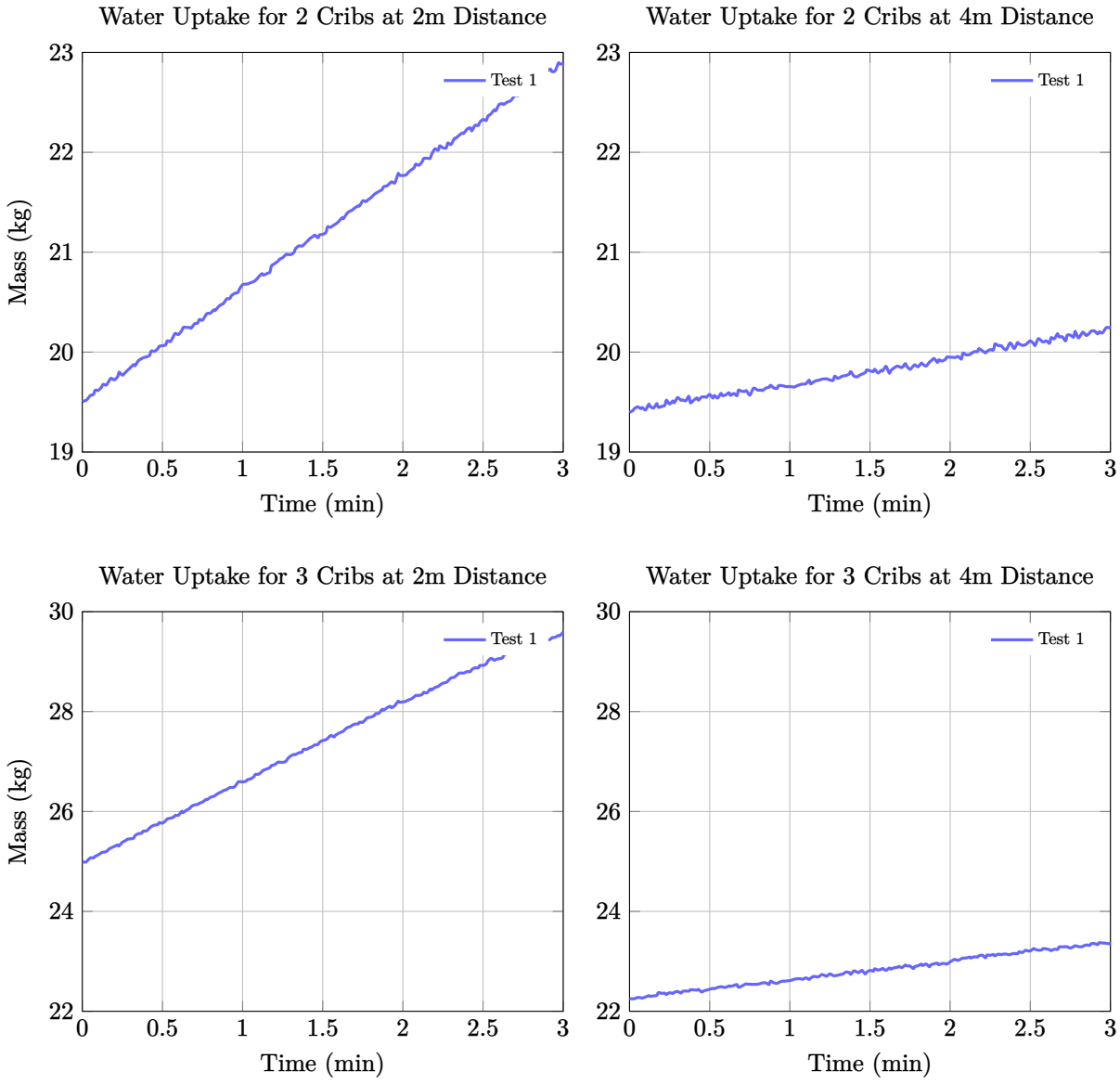

Figure B.1: Water Uptake over time at a 2- and 4-meter distance.